Dlg1 controls planar spindle orientation in the neuroepithelium through direct interaction with LGN

Mehdi Saadaoui,[1,2,3] Mickaël Machicoane,[4,5,6] Florencia di Pietro,[1,2,3,7] Fred Etoc,[1,2,3] Arnaud Echard,[4,5] and Xavier Morin[1,2,3]

[1]Institut de Biologie de l'École Normale Supérieure, Ecole Normale Supérieure, F-75005 Paris, France
[2]Institut National de la Santé et de la Recherche Medicale, U1024, F-75005 Paris, France
[3]Centre National de la Recherche Scientifique, Unité Mixte de Recherche 8197, F-75005 Paris, France
[4]Membrane Traffic and Cell Division Laboratory, Institut Pasteur, F-75015 Paris, France
[5]Centre National de la Recherche Scientifique, Unité de Recherche Associée 2582, F-75015 Paris, France
[6]Cellule Pasteur–Université Pierre et Marie Curie, Université Pierre et Marie Curie, F-75015 Paris, France
[7]Institute of Doctoral Studies (IFD), Sorbonne Universités, Université Pierre et Marie Curie–Université Paris 6, F-75252 Paris, France

Oriented cell divisions are necessary for the development of epithelial structures. Mitotic spindle orientation requires the precise localization of force generators at the cell cortex via the evolutionarily conserved LGN complex. However, polarity cues acting upstream of this complex in vivo in the vertebrate epithelia remain unknown. In this paper, we show that Dlg1 is localized at the basolateral cell cortex during mitosis and is necessary for planar spindle orientation in the chick neuroepithelium. Live imaging revealed that Dlg1 is required for directed spindle movements during metaphase. Mechanistically, we show that direct interaction between Dlg1 and LGN promotes cortical localization of the LGN complex. Furthermore, in human cells dividing on adhesive micropatterns, homogenously localized Dlg1 recruited LGN to the mitotic cortex and was also necessary for proper spindle orientation. We propose that Dlg1 acts primarily to recruit LGN to the cortex and that Dlg1 localization may additionally provide instructive cues for spindle orientation.

Introduction

Oriented cell divisions play a crucial role in the development, growth, and homeostasis of many tissues (Morin and Bellaïche, 2011). Divisions within the plane of epithelial structures (thereafter referred to as planar divisions) both contribute to the expansion of the tissue surface and are essential for tissue integrity through maintenance of the epithelial monolayer organization (Fleming et al., 2007). Conversely, divisions perpendicular to the epithelial plane (vertical divisions) have been shown to contribute to tissue stratification, binary fate decisions, and regulation of stem cell pools (Quyn et al., 2010; Williams et al., 2011). Defective control of spindle orientation leads to developmental and homeostasis defects and may be a step in the transformation process leading to cancer (Pease and Tirnauer, 2011; Noatynska et al., 2012).

In many models of oriented cell divisions, spindle orientation relies on the specific cortical subcellular localization of a core molecular complex composed of the $G\alpha_i$ subunits of heterotrimeric inhibitory G proteins, of LGN (also referred to as G protein–signaling molecule 2 and as Pins in *Drosophila melanogaster*), and of nuclear mitotic apparatus (NuMA). This LGN complex recruits motor proteins (cytoplasmic dynein and its regulators) to concentrate force generators that pull on astral microtubules to position and orient the mitotic spindle along a specific axis (Morin and Bellaïche, 2011). Apical distribution of the LGN complex is required for vertical spindle orientation in the asymmetric division of both *Drosophila* neuroblasts (NBs; Yu et al., 2000) and mouse embryonic skin progenitors (Lechler and Fuchs, 2005; Williams et al., 2011), whereas its lateral enrichment controls planar spindle orientation in vertebrate neuroepithelial and MDCK cells (Zheng et al., 2010; Peyre et al., 2011).

Correspondence to Xavier Morin: xavier.morin@ens.fr

F. Etoc's present address is Center for Studies in Physics and Biology and Laboratory of Molecular Vertebrate Embryology, The Rockefeller University, New York, NY 10065.

Abbreviations used in this paper: aPKC, atypical PKC; Dlg, discs large; GPR, G protein regulatory; GUK, guanylate kinase; Insc, Inscuteable; LR, linker region; NB, neuroblast; NuMA, nuclear mitotic apparatus; PACT, Pericentrin/AKAP-450 centrosomal targeting.

The Rockefeller University Press $30.00
J. Cell Biol. Vol. 206 No. 6 707–717
www.jcb.org/cgi/doi/10.1083/jcb.201405060

The LGN complex appears as a generic cog in spindle orientation, taking orders from intra- and extracellular upstream polarity cues. In *Drosophila* NBs, positional information is given by the apically located Par complex, which recruits the LGN complex via the Inscuteable (Insc) adapter protein (Morin and Bellaïche, 2011). Likewise, in mouse embryonic skin progenitors, integrin signaling from the basal lamina acts as a positional cue for intracellular Par-Insc-LGN localization at the apical cell cortex to promote vertical spindle orientation and skin stratification (Lechler and Fuchs, 2005; Williams et al., 2011). Insc also controls vertical and oblique spindle orientation at the expense of planar divisions in the vertebrate neuroepithelium (Žigman et al., 2005; Postiglione et al., 2011).

Polarity cues driving planar spindle orientation in vertebrate epithelia are poorly understood, and the mechanism responsible for the lateral restriction of LGN in dividing cells (Zheng et al., 2010; Peyre et al., 2011) is unclear. Experiments in 3D culture of MDCK cells indicated that apical atypical PKC (aPKC) phosphorylates LGN, locally increasing LGN affinity with a 14–3-3 protein that competes with $G\alpha_i$ for LGN interaction, thereby excluding LGN from the apical cortex (Hao et al., 2010). Although a similar role of aPKC was observed in *Drosophila* larval wing disk epithelia (Guilgur et al., 2012), it does not seem to be the case in the chick neuroepithelium (Peyre et al., 2011). Studies in *Drosophila* suggested a role of the discs large (Dlg) gene family: *dlg* mutant sensory organ precursors show defective spindle orientation and reduced accumulation of Pins at the anterior cell cortex in *Drosophila* larvae (Bellaïche et al., 2001). Dlg is also part of a nonessential microtubule-based pathway driving cortical localization of LGN–$G\alpha_i$ in fly NBs (Siegrist and Doe, 2005; Johnston et al., 2009). Finally, defects in spindle orientation were recently described in *Drosophila dlg* mutant larval wing disks and adult female follicular cells (Bergstralh et al., 2013; Nakajima et al., 2013). In vitro studies have revealed biochemical interactions between LGN and several members of the Dlg family, but the functional relevance of this interaction has not been investigated in vivo (Sans et al., 2005; Johnston et al., 2009; Zhu et al., 2011).

Here, we show that vertebrate Dlg1/SAP97 (Synapse-associated protein 97) is polarized at the mitotic cell cortex and is essential for directional movements, resulting in planar spindle orientation in the chick neuroepithelium. Using point mutations in both Dlg1 and LGN, we demonstrate that the direct interaction between Dlg1 and LGN plays a key role in LGN cortical recruitment and spindle orientation in vivo. We further show that Dlg1 also controls LGN cortical accumulation and substrate-induced spindle orientation in cells cultured on adhesive micropatterns. Our data reveal a major function for Dlg1 in recruiting LGN to the mitotic cortex and in proper spindle orientation in multiple cellular contexts in vertebrates.

Results and discussion

Dlg1 is required for planar spindle orientation in chick neural progenitors

We focused on chick Dlg1/SAP97/Dlh: among the four DLG family members found in chick databases, Dlg1 is structurally the most closely related to canonical *Caenorhabditis elegans* dlg-1 and *Drosophila* Dlg (Assémat et al., 2008) and was found expressed in the chick neural tube at E3 (Fig. S1 A). Interestingly, a GFP-Dlg1 fusion protein was enriched at the basolateral cell cortex during mitosis upon in ovo electroporation in the chick neuroepithelium (Fig. 1, A and B; and Fig. S2 for a list of vectors used in this study).

We addressed a possible role of Dlg1 in spindle orientation using miRNA-based RNAi vectors (Das et al., 2006). Silencing efficiency was assessed by the loss of GFP-Dlg1 fusion expression (Fig. S1 B). We measured spindle orientation in en face views of flat mounted neural tubes (Figs. 1 A and S1 C; Materials and methods). Although the majority of control cells exhibited a planar orientation both in metaphase ($\alpha_{mean\ Ctrl}$ = 11.9°, n = 85) and anaphase ($\alpha_{mean\ Ctrl}$ = 8.3°, n = 51; Fig. 1, C and D), cells expressing Dlg1 miRNA showed a misoriented spindle in metaphase ($\alpha_{mean\ Dlg-}$ = 29.3°, n = 106, P < 0.0001) and, to a minor extent, in anaphase ($\alpha_{mean\ Dlg-}$ = 12.8°, n = 59, P = 0.0048; Fig. 1, C and D).

Drosophila Dlg is important for adherens junction structure and cell polarity in interphase cells (Woods and Bryant, 1991), and a similar role has been proposed for Dlg1 based on siRNA experiments in cultured human epithelial cells (Laprise et al., 2004). However, analysis of Dlg1 mouse mutant phenotypes in the embryonic lens and urogenital tracts did not reveal a general requirement for Dlg1 in epithelial polarity (Naim et al., 2005; Mahoney et al., 2006; Iizuka-Kogo et al., 2007; Rivera et al., 2009), although specific cell types in the lens show cell-autonomous polarity defects (Rivera et al., 2009). We investigated whether Dlg1 knockdown may disrupt cell polarity in the neuroepithelium at different time points after electroporation. Remarkably, overall tissue organization was not perturbed (Fig. 1 E, top). Subapical localization of the tight junction marker ZO-1 (Figs. 1 E and S1 D) and apical distribution of aPKC (Fig. S1 E) were not affected, even after a long period of RNAi treatment. In addition, subapical enrichment of the adherens junction markers N-cadherin and β-catenin was undistinguishable from control cells (Figs. 1 E and S1 D). Hence, Dlg1 is not required for the maintenance of cell polarity and has an essential role in planar spindle orientation of neuroepithelial cells in vivo.

Mitotic spindle movements are randomized in Dlg1 knockdown cells

To understand why Dlg1 is essential for spindle orientation, we analyzed spindle dynamics in Dlg1-depleted cells. Chick embryos were electroporated with fluorescent reporters to label centrosomes and chromosomes in control or Dlg1 RNAi–expressing cells. We imaged the neuroepithelium using an en face culture protocol (Peyre et al., 2011) and designed a semi-automated 3D centrosome-tracking routine (Materials and methods; Fig. 2 A) to analyze the behavior of dividing cells. In both control and Dlg1-depleted cells, mean spindle orientations relative to the apical surface were similar to those observed in fixed conditions in metaphase and anaphase cells (Fig. 2 B). We concentrated on spindle movements relative to the apicobasal axis (z axis in the en face view). During prophase, the two

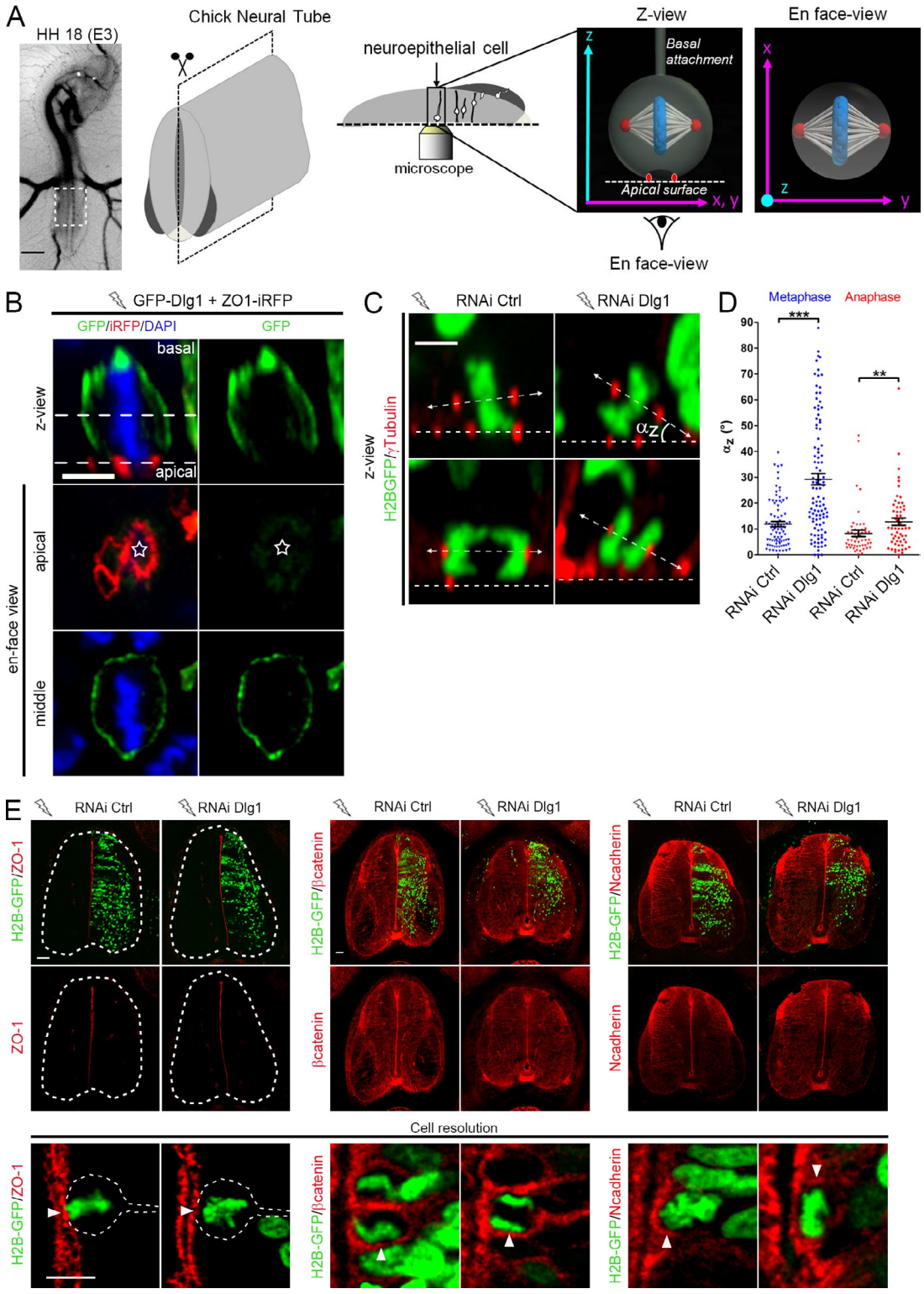

Figure 1. **Dlg1 is required for planar spindle orientation in chick neural progenitors.** (A) Scheme of flat mounting of the E3 (Hamburger Hamilton [HH] stage 18) chick neural tube for en face imaging of neuroepithelial cells. (B) GFP-Dlg1 is restricted to the basolateral cortex during metaphase. The z view is a reslice along the z axis of the confocal stack acquired in en face view. The four bottom images show single optical sections from the en face view (apical and middle levels). ZO-1 (red) labels tight junctions. White dashed lines on the z view show focal planes chosen for the apical and middle en face views. White stars show apical domain of the GFP-Dlg1–expressing cell. (C) Z view along the axis of the mitotic spindle of metaphase and anaphase cells expressing control (Ctrl) or Dlg1-targeting miRNAs (H2B-GFP marker). H2B-GFP and γ-tubulin label chromosomes and spindle poles, respectively. (D) Quantification of mitotic spindle α_z orientation at E3, 24 h after electroporation (means ± SEM, $n > 50$ cells from at least three embryos). **, $P \leq 0.01$; ***, $P \leq 0.001$. (E) Tissue architecture (top) and apicobasal polarity (cell resolution images) are not affected in neural tubes electroporated with Dlg1 miRNA as illustrated by ZO-1, β-catenin, or N-cadherin staining. White arrowheads point to H2B-GFP–positive electroporated cells. Dotted lines highlight the contour of the neural tube (top) or of individual dividing cells (bottom). Bars: (A) 1.5 mm; (B and C) 5 µm; (E, top) 50 µm; (E, bottom) 10 µm.

centrosomes disengage from the apical surface and move to two opposite sides of the nucleus and form the bipolar spindle upon nuclear envelope breakdown during prometaphase. The distance between spindle poles remains stable during prometaphase and metaphase and until anaphase onset. We used this distance as a means to stage progression through mitotic phases. In control cells, the mitotic spindle formed with a random orientation relative to the z axis (Fig. 2 C; Peyre et al., 2011). Within 5 min, it underwent a phase of directed z rotation away from this axis to align parallel to the apical surface. During a second phase, it remained in the planar orientation, while displaying oscillatory z rotations (Fig. 2, C and E; and Video 1). Dlg1 RNAi cells failed to undergo the directed z rotation that occurs immediately after spindle formation. Instead, spindles experienced random movements relative to the z axis throughout prometaphase and metaphase. This led to a nonplanar orientation at anaphase onset (Fig. 2, D and E; and Video 2). The ability of the spindle to move was not impaired because the absolute z rotation in 1-min intervals (our time frame in these experiments) was not different from control cells (Fig. 2 F). However, whereas control cells showed a specific directional bias of spindle movements away from the apicobasal axis during early metaphase (relative rotation $\delta_{z(t_{1-5})} = -6 \pm 1.4°/\text{min}$; Fig. 2 G), this bias was lost in Dlg1-depleted cells ($\delta_{z(t_{1-5})} = -1 \pm 1.3°/\text{min}$, $P = 0.0025$; Fig. 2 G). Hence, defective spindle orientation upon Dlg1 knockdown results from a failure to orient their rotation movement toward the planar orientation in early metaphase, rather than from an inability to rotate.

Dlg1 is required to orient the spindle in dissociated cells cultured on adhesive micropatterns

We then explored whether Dlg1 is also involved in spindle orientation in a nonepithelial context. In vitro, adherent cells typically divide parallel to the plane of the culture dish. We found that Dlg1-depleted HeLa cells displayed a slightly tilted angle in metaphase compared with controls ($\alpha_{z\ Dlg-} = 10.6°$ and $\alpha_{z\ Ctrl} = 5.9°$, $P = 0.0037$; Fig. 3 A). This defect was absent in anaphase, suggesting that planar orientation is delayed upon Dlg1 silencing ($\alpha_{z\ Dlg-}$ and $\alpha_{z\ Ctrl} = 5.4°$; Fig. 3 A). To investigate whether Dlg1 might be involved in spindle orientation in the xy plane, which depends on the geometry of cell adhesion to the substrate (Théry et al., 2005, 2007), we used cells cultured on L shape adhesive micropatterns. In this system, the mitotic spindle predominantly aligns with the hypotenuse of the triangle defined by the L shape (Fig. 3 B; Théry et al., 2005). Remarkably, Dlg1 distribution in the xy plane was homogeneous at the cell cortex of prometaphase and metaphase cells and did not display any enrichment relative to the spindle poles or the pattern geometry (Fig. 3 B). Control cells displayed a spindle angle distribution tightly centered on 45° at anaphase onset, as expected (Fig. 3 C). In contrast, Dlg1-depleted cells showed a significantly broader angle distribution, with a twofold reduction in the number of spindles correctly oriented at 45° (23 ± 3% of Dlg1 RNAi vs. 42 ± 6% of control cells in the 15° bin centered on 45° [$P < 0.0001$ and $D = 0.124$]; Fig. 3 C).

In control cells, the spindle is only loosely oriented at the beginning of mitosis and undergoes directed rotation movements toward the 45° orientation mainly during late prometaphase and early metaphase (Machicoane et al., 2014). The final orientation is typically reached within 15 min after metaphase onset and maintained until anaphase (Fig. 3 D). In contrast, we observed that directed rotation toward the 45° position was reduced in Dlg1-depleted cells, with movements of the spindle essentially consisting in oscillations around its initial position (Fig. 3 D).

Hence, directed spindle rotation in the xy plane during metaphase is also compromised by Dlg1 knockdown in HeLa cells cultured on adhesive micropatterns. However, in this system, Dlg1 is homogeneous at the cortex, suggesting that its localization is not instructive. Rather, its role may be permissive, allowing cells to translate cues from the adhesive pattern into a specific spindle orientation.

LGN cortical localization depends on Dlg1

Direct biochemical interactions have been described between the C-terminal guanylate kinase (GUK) domain of several Dlg family members and the central linker region (LR) domain of LGN (Figs. 3 E and 4 A; Sans et al., 2005; Johnston et al., 2009; Zhu et al., 2011). Because LGN is essential for spindle orientation, the defects observed upon Dlg1 depletion in both chick and HeLa cells might be a result of a direct effect on LGN. We thus investigated the distribution of LGN after Dlg1 knockdown.

In HeLa cells in metaphase, LGN appeared as two cortical crescents with a symmetric distribution facing the spindle poles, as expected (Kiyomitsu and Cheeseman, 2012). In contrast, after Dlg1 depletion, cortical levels of LGN were decreased, and the remaining cortical LGN was distributed evenly (Fig. 3 E). Cortical localization of NuMA in metaphase relies on LGN (Peyre et al., 2011; Kiyomitsu and Cheeseman, 2013). Accordingly, NuMA was lost from the cortex in Dlg1-depleted cells, whereas it was still visible on the spindle (Fig. 3 E).

Similarly, in Dlg1-depleted cells in vivo, a GFP-LGN fusion no longer accumulated at the lateral cell cortex, with a twofold decrease of the cortical over cytoplasmic signals in metaphase compared with control cells (Fig. 4 B). Conversely, LGN knockdown did not prevent the cortical distribution of a GFP-Dlg1 fusion protein (Fig. S3 A).

Altogether, we conclude that Dlg1 acts upstream of LGN/NuMA and is essential for the cortical recruitment of LGN. In cultured cells, Dlg1 is homogenous at the cortex and therefore likely permissive for the cell to respond to external orientation cues provided by adhesive micropatterns. In epithelia, the apicobasal polarization of Dlg1 distribution may additionally provide an instructive cue for planar orientation.

Direct LGN–Dlg1 interaction is necessary for mitotic spindle orientation

Dlg1 involvement in LGN localization led us to dissect the functional domains of LGN necessary for its cortical distribution. Because LGN is also known to interact with cortically anchored GDP-bound $G\alpha_i$ subunits via the four G protein regulatory (GPR) domains located at its C terminus (Fig. 4 A; Willard et al., 2004; Morin et al., 2007; Peyre et al., 2011), we addressed the specific requirement of LGN binding domains

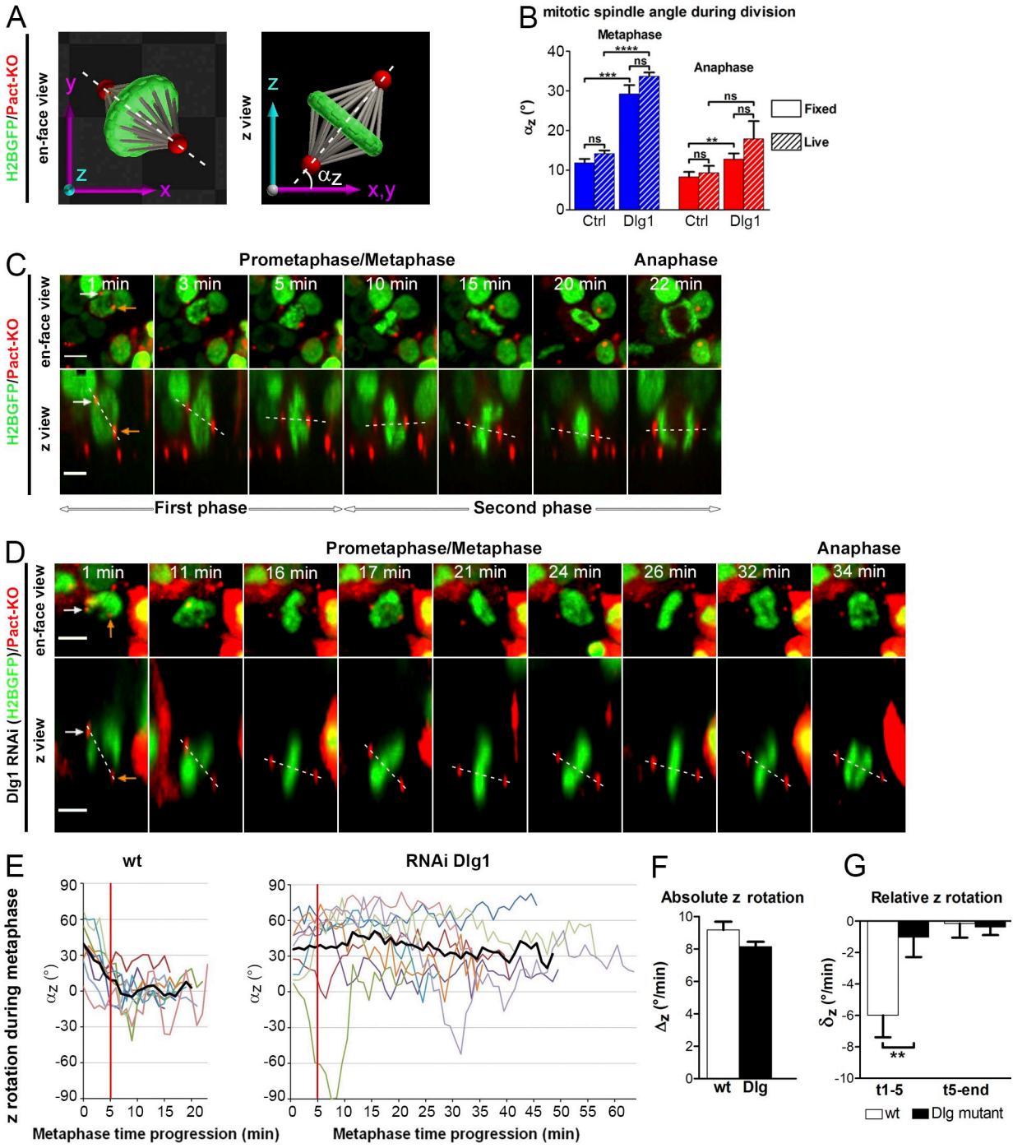

Figure 2. **Mitotic spindle movements are randomized in Dlg1 knockdown cells.** (A) 3D models of a mitotic neuroepithelial cell imaged from the apical surface (xy plane) or seen along its apical–basal axis (z axis). α_z represents the angle between the spindle axis and the apical (xy) plane. (B) Mitotic spindle α_z measurements reveal an identical phenotype in Dlg1 knockdown between fixed and live conditions. For metaphase measurements, $n = 206$ time frames from 13 control (Ctrl) cells and 574 time frames from 15 Dlg RNAi cells. Error bars show SEMs. (C and D) Time-lapse series of dividing neuroepithelial cells expressing PACT-mKO1 (PACT-KO) and H2B-GFP without (C) or with (D) Dlg1 RNAi. (top) En face view projection of z stacks encompassing both centrosomes. (bottom) Vertical z section along the mitotic spindle axis. White and orange arrows point to the same centrosome in en face and z views. Dotted lines highlight the spindle axis. Bars, 5 µm. (E) Z rotation dynamics during metaphase for control cells (left) or Dlg1 RNAi cells (right). Each color curve corresponds to one individual cell (nine representative cells). Thick black lines show mean angles of all analyzed cells normalized to metaphase onset. The red lines mark the time of the transition from the phase of directed z rotation to the phase of planar maintenance observed in control cells. (F and G) Absolute and relative (directional) z rotations (means + SEM) for control (F) and Dlg1 RNAi cells (G). See Materials and methods for a definition of absolute and relative rotation. wt, wild type. **, $P \leq 0.01$; ***, $P \leq 0.001$; ****, $P \leq 0.0001$.

to $G\alpha_i$ and Dlg1 in its cortical localization through analysis of the localization of GFP-tagged truncated forms of LGN. Individually, LGN linker (LR) and GPR domains were detectable at the cell cortex over a strong cytoplasmic signal. In contrast, combining both domains (LR-GPR) led to a much stronger and almost exclusive cortical localization (Fig. 4 C).

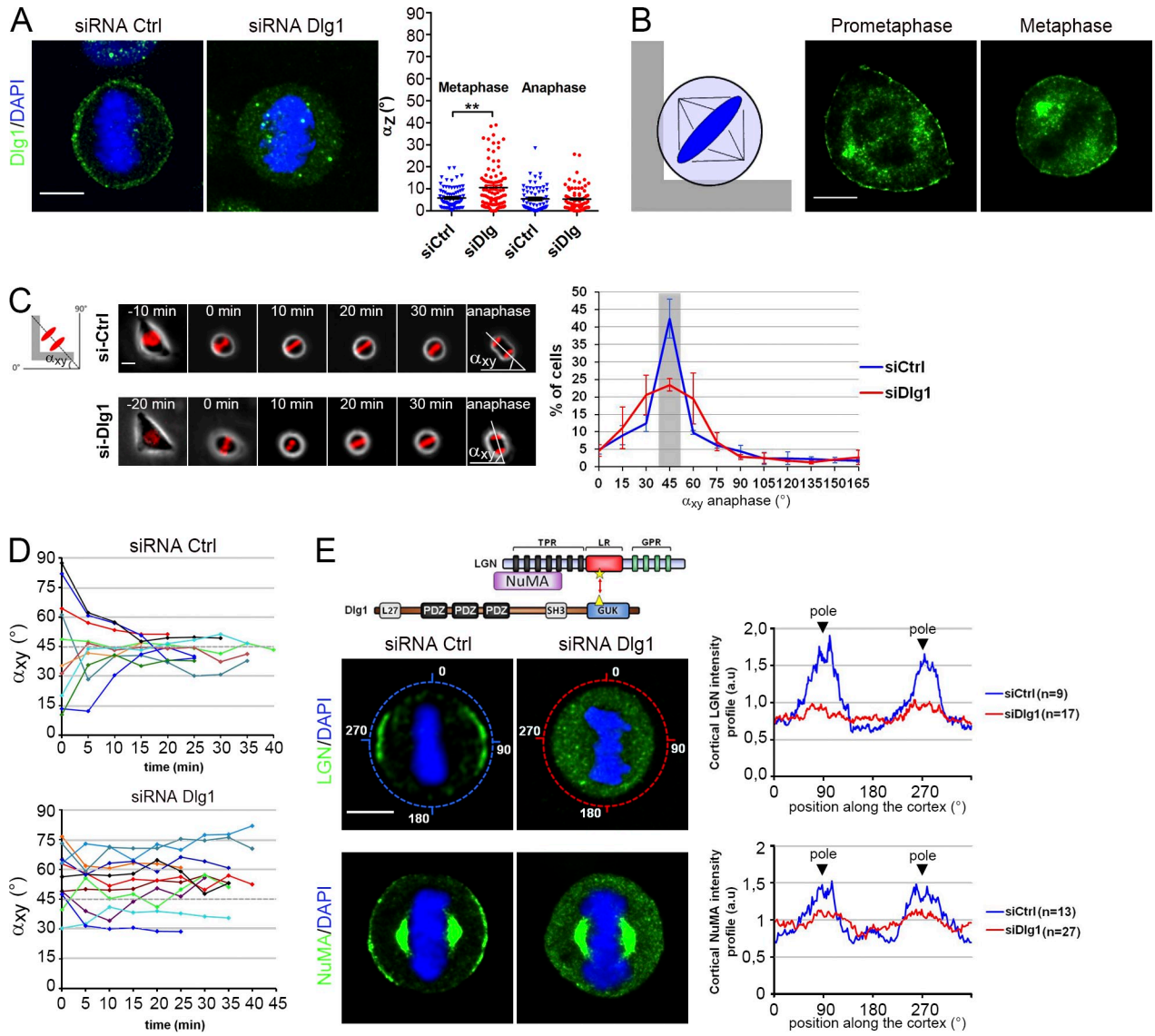

Figure 3. **Dlg1 is required to orient the spindle in dissociated cells cultured on adhesive micropatterns.** (A, left) Cortical localization of Dlg1 in HeLa cells cultured on nonpatterned coverslips. Dlg1 staining was lost upon siRNA treatment. (right) Distribution of the mitotic spindle angles relative to the coverslip in control and Dlg1 RNAi cells (α_z, means ± SEM, $n > 70$ cells). **, $P \leq 0.01$. (B) Cortical localization of Dlg1 during prometaphase and metaphase in cells cultured on L shape fibronectin micropatterns, as schematized on the left. (C) Control and Dlg1 siRNA–treated H2B-Cherry–expressing HeLa cells were cultured on L shape patterns and recorded by time-lapse microscopy. (left) Representative examples of time-lapse sequences of control or siDlg1 cells. A scheme of L shape micropattern and orientation of the mitotic spindle at anaphase onset is provided. (right) Distribution of mitotic spindle angles relative to pattern orientation (α_{xy}) at anaphase onset (means ± SD, $n > 750$ cells from three independent experiments). The gray box highlights the 15° bin centered around 45°. (D) Evolution of the mitotic spindle α_{xy} orientation during mitosis plotted for a dozen cells from C. (E, top left) Dlg1–LGN–NuMA interacting domains. Yellow star and triangle represent amino acids necessary for Dlg1–LGN interaction: P769 in Dlg1 and S401 in LGN, respectively. (bottom left) Confocal slices of nonpatterned control and Dlg1 siRNA–transfected metaphase cells stained for LGN and NuMA. (right) Graph showing mean LGN and NuMA cortical intensity profiles for control and Dlg1 siRNA–treated cells. Cortical coordinates along the plot correspond to the blue and red circles depicted in the LGN images. a.u., arbitrary unit; Ctrl, control; TPR, tetratricopeptide repeat; PDZ, PSD95/Dlg/ZO-1 domain. Bars: (A, B, and E) 10 µm; (C) 5 µm.

In vitro, phosphorylation of a serine residue corresponding to S401 of LGN increases by 500-fold the affinity of a peptide located in the LGN LR toward purified Dlg1 (Zhu et al., 2011). Interestingly, substitution of an alanine at this position reduced the cortical enrichment of the LR-GPR GFP fusion in vivo (S401A; Fig. 4 D). Together, these results show that Dlg1–LGN and $G\alpha_i$–LGN interactions are both required for proper cortical localization of LGN during division.

To confirm the role of Dlg1–LGN interaction in LGN localization by another approach, we overexpressed the LGN interacting domain of Dlg1 (GUK domain; Fig. 4 A) together with GFP-LGN in neuroepithelial cells. As anticipated, the GUK domain behaved as a dominant negative that displaced GFP-LGN from the cell cortex and caused spindle orientation defects (Fig. S3, B and C). In *Drosophila*, the interaction between Dlg and the Pins linker depends on a conserved proline residue in the GUK domain (Johnston et al., 2011). Accordingly, substitution of this proline for a serine residue in the chick Dlg1 GUK domain abolished its dominant-negative effect on LGN cortical localization and spindle orientation (Fig. S3, B and C).

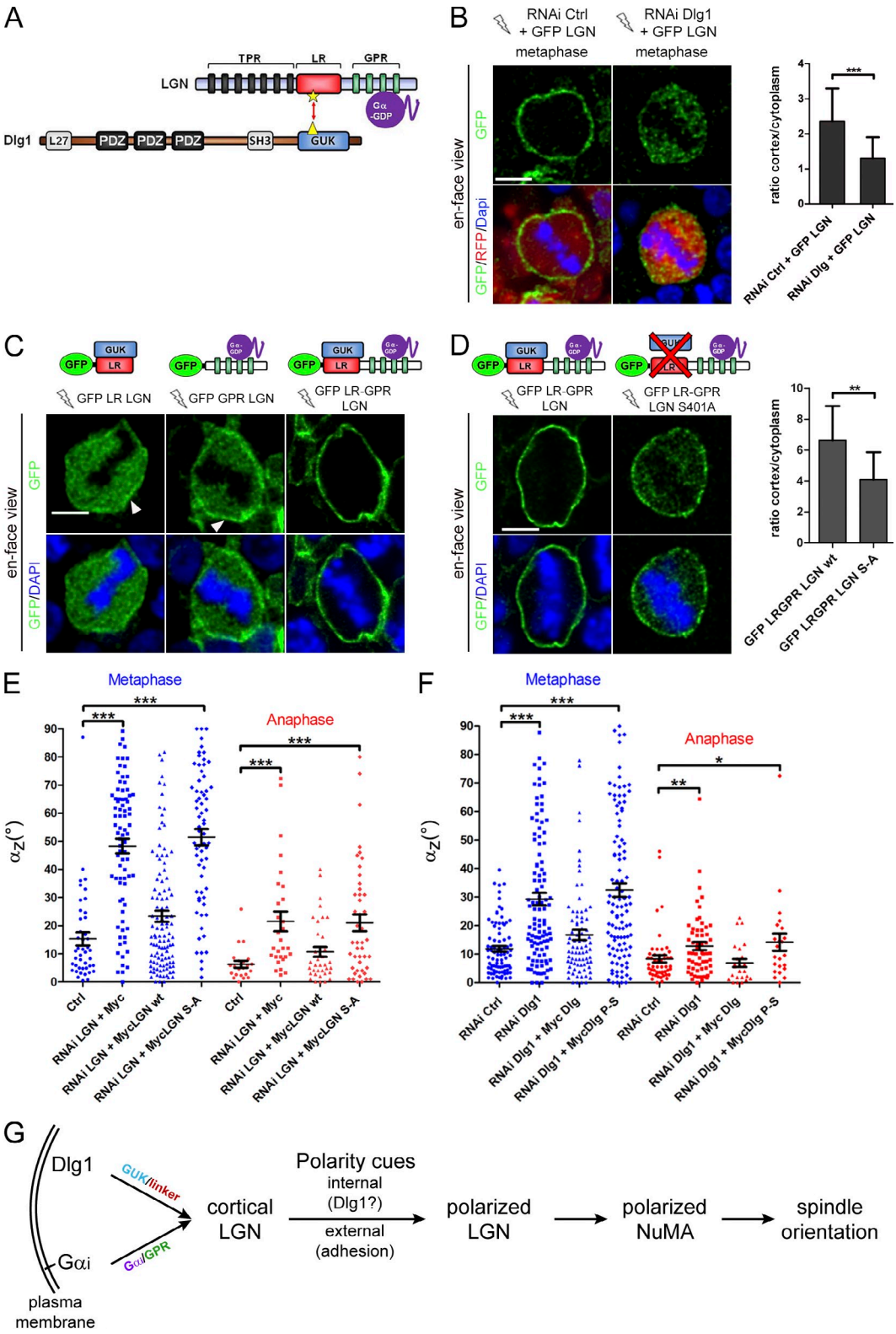

Figure 4. **Direct LGN–Dlg1 interaction is necessary for LGN cortical localization and mitotic spindle orientation.** (A) Dlg1–LGN–$G\alpha_i$ functional domains. TPR, tetratricopeptide repeat; PDZ, PSD95/Dlg/ZO-1 domain. (B) GFP-LGN recruitment to the cell cortex is reduced upon Dlg1 RNAi (cytoplasmic RFP marker). (C) Localization of GFP fusions to linker (LR), GPR, and LR + GPR domains of LGN in E3 chick neural progenitors. White arrowheads point the weak cortical localization of the LR and GPR domains. (D) Serine at position 401 in LGN is necessary for the additive effect of the LR domain in LR-GPR cortical recruitment. Graphs in B and D show ratios of cortical over cytoplasmic GFP signals (means + SEM, $n > 15$ cells). (E and F) Mitotic spindle angle distribution in metaphase and anaphase for RNAi rescue experiments (means ± SEM). (G) $G\alpha_i$ and Dlg1 cooperate for LGN cortical recruitment and/or stabilization. Instructive polarity cues, either external (adhesion to substrate) or cell autonomous (possibly involving Dlg1 localization), and control LGN and NuMA polarization, resulting in spindle orientation, are depicted. It is not known whether Dlg1 and $G\alpha_i$ are mutually dependent for their cortical localization. Ctrl, control; wt, wild type. *, $P \leq 0.05$; **, $P \leq 0.01$; ***, $P \leq 0.001$. Bars, 5 µm.

To demonstrate that the mutual interaction between Dlg1 and LGN is necessary for spindle orientation, we performed RNAi rescue experiments in vivo using RNAi-resistant forms of LGN and Dlg1. Whereas wild-type mouse LGN displayed a clear cortical localization and efficiently rescued spindle orientation defects caused by chick LGN knockdown, mouse LGN-S401A was poorly recruited to the cortex (Fig. S3 D) and, accordingly, did not rescue spindle orientation (Fig. 4 E). Similarly, a full-length RNAi-resistant Dlg1 rescued both LGN-GFP cortical localization and spindle orientation defects caused by Dlg1 knockdown, whereas these defects were not rescued by the mutant version of full-length Dlg1 with a proline to serine substitution in the GUK domain (Figs. S3 E and 4 F). Hence, point mutations that suppress the direct interaction between Dlg1 and LGN are sufficient to recapitulate the loss-of-function phenotypes in the neuroepithelium. We conclude that this direct interaction is necessary for their function in spindle orientation in vivo.

Our results show a requirement for Dlg in spindle orientation in a variety of cellular contexts. This may reveal an ancestral and possibly universal role for the Dlg/LGN pair, which may even predate the involvement of Dlg in apicobasal polarity that has so far attracted most of the interest. In the light of the present study, it will be interesting to determine whether and how Dlg1 controls spindle orientation in cell types that undergo developmentally regulated switches between planar and vertical modes of division, such as skin progenitors and intestinal or mammary stem cells (Lechler and Fuchs, 2005; Quyn et al., 2010; Williams et al., 2011; Elias et al., 2014).

Materials and methods

Electroporation and plasmids

Electroporation in the chick neural tube was performed at embryonic day 2 (E2) as described previously (Morin et al., 2007). For gain- or loss-of-function experiments, plasmids were used at 1 µg/µl. For rescue experiments, 6-Myc–tagged LGN and Dlg1 expression constructs under the CAGGS promoter were added at 0.2 µg/µl. Mouse and chick LGNs are very closely related, and GFP-tagged versions of the two proteins display identical subcellular distribution (this study; Peyre et al., 2011); besides, mouse LGN was previously shown to be able to substitute for both chick LGN and *Drosophila* Pins (Yu et al., 2003; Morin et al., 2007). We therefore used mouse LGN to investigate cortical recruitment and to rescue chick LGN RNAi phenotypes. For Dlg1 RNAi rescue experiments, an RNAi-resistant 6-Myc–tagged chick Dlg1 construct was generated by targeted mutagenesis, introducing five silent base substitutions in the region targeted by the Dlg1 1135 miRNA construct. GFP-tagged LGN and Dlg1 expression constructs under the cytomegalovirus promoter were used at 1 µg/µl. Full-length cDNA of chick Dlg1-SAP97 and short cDNA of Dlg1, 2, and 3 and GAPDH used in RT-PCR experiments were amplified from chick neural tube cDNA samples prepared with the first-strand synthesis system (SuperScript III; Invitrogen). Several targets were chosen to down-regulate chick Dlg1 according to described recommendations (Das et al., 2006). The most effective construct was Dlg1 1135, which targets bases 1,135–1,155 in the Dlg1 cDNA: 5′-TTAGAAGAAGTTACTCATGAA-3′. Expression vectors used in this study are listed in Fig. S2. Pericentrin/AKAP-450 centrosomal targeting (PACT)–mKO1 was a gift from F. Matsuzaki (RIKEN Center for Developmental Biology, Kobe, Japan).

Immunohistochemistry

For antibody staining, chick embryos were fixed for 1 h in ice-cold 4% formaldehyde/PBS. For cryosections, embryos were washed three times in 0.12 M phosphate buffer (PB), pH 7.2, and equilibrated overnight at 4°C in PB/15% sucrose. Embryos were then embedded in PB/15% sucrose/7.5% gelatin for cryoprotection before sectioning. Before immunostaining, cryosections were equilibrated at RT, degelatinized in PBS at 37°C for 5 min, and permeabilized 10 min in PBS/0.1% Triton X-100 (PBT 0.1%) before a 30-min blocking step in PBT 0.1%/10% FCS. For en face views, embryos were cut along their midline and permeabilized for 15 min in PBS/0.3% Triton X-100 (PBT 0.3%) before a 1-h blocking step in PBT 0.3%/10% FCS. For cell culture, HeLa cells were fixed for 20 min at RT in 4% formaldehyde/PBS, rinsed with PBS, and permeabilized in PBT 0.1% for 5 min.

Primary antibodies used in this study are mouse anti-GFP (Torrey Pines Biolabs), mouse anti–γ-tubulin (clone GTU-88), mouse anti–c-Myc (clone 9E10), rabbit anti–c-Myc, mouse anti–N-cadherin (clone GC-4) obtained from Sigma-Aldrich, mouse anti–ZO-1 (Invitrogen), mouse anti–β-catenin (BD), rabbit anti–aPKC-ζ (sc-206), rabbit anti-Dlg1 (sc-25661) from Santa Cruz Biotechnology, Inc., and rabbit anti-LGN (a gift from F. Matsuzaki). For the γ-tubulin antibody, embryos were incubated for 5 min in 100% acetone preequilibrated at −20°C and rinsed twice in PBS at RT before the blocking step. Secondary antibodies coupled to Alexa Fluor 488, Cy3, or Cy5 were obtained from Jackson ImmunoResearch Laboratories, Inc. and typically used at 1:400 dilutions. Vectashield with DAPI (Vector Laboratories) was used as a mounting medium.

Image acquisition

Optical sections of fixed samples (en face views from half-embryos or transverse views from cryosections) were obtained on a confocal microscope (SP5; Leica) using 20 and 40× (Plan Neofluar NA 1.3 oil immersion) objectives and LAS software (Leica). Fiji software (Schindelin et al., 2012) was used for images processing (Gaussian blur) and data analysis (spindle orientation measurement). When necessary, images were subjected to brightness and contrast adjustment to equilibrate channel intensities and background using Photoshop CS4 software (Adobe).

3D measurement of spindle orientation in fixed samples

Spindle orientation was measured on en face mounted neural tubes from E3 embryos labeled with an anti–γ-tubulin antibody to reveal spindle poles and with DAPI dye to label chromosomes. Electroporated cells were identified by their expression of a Histone2B-GFP reporter protein (carried by the miRNA plasmid), also revealing the chromosomal plate of dividing cells. In addition, for rescue and dominant-negative experiments (Figs. 4, E and F; and S4 C), expression of Myc-tagged expression constructs was revealed by an anti-Myc antibody. En face image stacks (0.5-µm z interval) were acquired at 40× magnification. Z views and spindle orientation quantification were performed in Fiji software (Schindelin et al., 2012) using custom-designed macros. Scrolling through the z levels, the x and y position of both centrosomes of all metaphase and anaphase cells in a field were recorded using the Point tool in ImageJ/Fiji (National Institutes of Health) with Add to ROI Manager selected. A custom-written ImageJ/Fiji macro was used to treat all cells as a batch as follows (zip file 1): for each cell, xy coordinates were used to define a 100-pixel-long line joining both centrosomes and centered on the midpoint between them. A resliced stack of five parallel images centered on this line (0.25-µm interval) was generated and projected (Z Projection tool with Max Intensity setting) to generate a single image of 1-µm-thick volume along the spindle axis. Images of all these cells were then assembled in a montage (one example is given in Fig. S2 C). Note that in each of the images, the apical surface is delineated by the position of subapical centrosomes located at the basis of the cilium of neighboring interphase cells. For each cell in the montage, four points were then defined and recorded as follows: first, two points defining the apical surface (typically corresponding to two apical centrosomes in interphase cells) and two points defining the spindle axis (one point for each centrosome of the dividing cell). Using a custom-written macro, all cells in the montage were treated as a batch, and their spindle orientation was calculated as the angle between the line that joins the two first and the line that joins the two last points (in the 0–90° range).

Time-lapse microscopy and analysis of cultured chick neural tube

En face live imaging. En face culture of the embryonic neuroepithelium was performed at E3 (24 h after electroporation). After removal of extraembryonic membranes, embryos were transferred to 37°C F12 medium and slit along their midline from the hindbrain to the caudal end. The electroporated side of the neural tube was peeled off with dissection forceps and transferred in F12 medium to a glass-bottom culture dish. 200 µl of 1% agarose F12 medium (penicillin/streptomycin and 1 mM sodium pyruvate) preheated at 42°C was gently pipetted up and down several times

to soak the neural tubes. Excess medium was then removed so that the neural tubes would flatten with their apical surface adhering to the bottom of the dish, and an additional thin layer of agarose medium was then added on top. After agarose polymerization, the whole dish was covered with 3 ml liquid F12/penicillin/streptomycin/sodium pyruvate medium and transferred to 37°C for 1 h for recovery before imaging. Imaging was performed with a 40× water immersion objective (Apochromat LWD NA 1.15; Nikon) on an inverted microscope (Ti Eclipse; Nikon) equipped with a heating enclosure and a spinning-disk confocal head (CSU-X1; Yokogawa Electric Corporation). We recorded 30-µm-thick z stacks (1 µm between individual sections) at 1-min intervals for 4–6 h using MetaMorph software (Molecular Devices) and an electron-multiplying charge-coupled device camera (Evolve; Roper Scientific).

3D tracking of the centrosomes. Based on 4D imaging of mitotic cells expressing a centrosome reporter (PACT domain of pericentrin fused to mKO1; Konno et al., 2008), we implemented a homemade MATLAB routine (MathWorks, Inc.; zip file 2) to measure the three spatial coordinates x, y, and z of each centrosome during the time course of the division. The routine runs on regions of interest centered on single dividing cells that are manually selected and cropped (x, y, and temporal) beforehand from the full-length acquisition. In brief, our software uncouples tracking in the xy plane and tracking in the z direction, and both operations are performed successively. First, the user creates a maximum intensity projection in the xy plane for each z stack of the video and defines manually an intensity threshold to segment the signal arising from the centrosomes. This operation results in the segmentation of multiple clusters of bright pixels, two of them being the centrosomes from the cell of interest. Cluster positions are defined as the barycenter of the fluorescence signal in the pixels inside each cluster. Clusters smaller than 2 pixels typically correspond to noise or mislocalized reporter and are therefore filtered out and removed from the analysis. Tracking of each centrosome in the xy plane is performed successively by selecting in the first frame the cluster associated to the centriole of interest. Then, the software tracks its position in the following frame by choosing the closest cluster, repeats this operation frame by frame in the whole video, and finally returns the associated trajectory in the xy plane. To get a robust tracking method, we implemented a semimanual procedure to correct for tracking mistakes arising, for example, from the localization of a centrosome close to a bright fluorescent spot in the background of the cell, which can lead to an incorrect localization in the following frame. In this case, the user can come back to the frame where the error occurred and select the correct cluster associated to the centrosome being tracked. Once the tracking in the xy plane is performed for the pair of centrosomes, the x and y coordinates are used to slice the imaging volume in the vertical direction, in the plane linking both centrosomes. A video with the two centrosomes in the vertical direction is thus generated, and the same tracking procedure as presented before is used to get the z coordinate of each centrosome. At the end of the procedure, the spatial coordinates x(t), y(t), and z(t) are returned for each centrosome and used to compute for each time point the distance between centrosomes, α_{xy} (the angle of the projection of the spindle axis in the xy plane), α_z (the angle of the spindle axis relative to the xy plane), and the distance covered by each centrosome in the xy plane and along the z axis since the previous time point.

The relative and absolute z rotations calculated in early (t1–t5) and late (t5–end) metaphase presented in Fig. 2 (F and G) were calculated as follows for each cell, between two time points *i* and *j*:

$$\text{absolute z rotation per minute, } \Delta_{z(t_{ij})} = \frac{\sum_{t=i}^{j-1}\left|\alpha_{z(t+1)} - \alpha_{z(t)}\right|}{\Delta t_{ij}};$$

$$\text{relative z rotation per minute, } \delta_{z(t_{ij})} = \frac{\sum_{t=i}^{j-1}\left(\alpha_{z(t+1)} - \alpha_{z(t)}\right)}{\Delta t_{ij}}.$$

Cell culture and transfection

HeLa cells expressing mCherry-H2B were cultured as previously described (Fink et al., 2011). For siRNA transfections, cells were treated following the manufacturer's instructions using HiPerFect (QIAGEN) for 72 h. Coverslips with L shape micropatterns were prepared and used as described in Fink et al. (2011). In brief, coverslips were first covered with poly-L-lysine-g-polyethylene glycol to passivate the surface. After UV illumination through a mask destroying the poly-L-lysine-g-polyethylene glycol in the unprotected areas, fibronectin (Sigma-Aldrich) was added at 50 µg/ml for 1 h. Fibrinogen coupled to Cy5 (Molecular Probes) was added to fibronectin for pattern visualization.

Time-lapse microscopy and measurement of spindle orientation of HeLa cells on micropatterns

HeLa cells expressing mCherry-H2B plated on L shape micropatterns were placed in a 37°C chamber (Chamlide; Live Cell Instrument) equilibrated with 5% CO_2. Single cells were imaged every 5 min using an inverted microscope (Ti Eclipse) equipped with a 10× air objective. Mitotic plates were followed throughout mitosis using the mCherry channel. Spindle orientation was calculated in early anaphase based on the angle measured between separated chromosomes and the micropattern using the angle tool of ImageJ (Fig. 3 B).

Statistical analysis

Statistical analyses were performed using a Mann–Whitney test performed with Prism (GraphPad Software), except for HeLa cell α_{xy} measurements, in which a Kolmogorov–Smirnov test was performed.

Quantification of cortical signals in mitotic cells

The profiles of LGN or NuMA signal at the cell cortex of metaphase HeLa cells shown in Fig. 3 D were measured in Fiji software as follows: a 5-pixel-wide line (Freehand Line tool) was manually traced following the cell contour in a confocal optical section corresponding to the middle plane of the cell. The start (and finish) point of this circular line was chosen facing the chromosome plate on one side of the cell. Pixel values along the line were calculated using the Plot Profile tool (each value corresponds to the mean value of the 5 pixels on the line width). As the absolute length of the circular line varies from cell to cell as a function of cell diameter, we designed a macro that interpolates plot values to calculate a normalized set of 360 values along the line, where positions 0 and 180 face the equatorial plate and positions 90 and 270 face the spindle poles, as illustrated in Fig. 3 D. For control and Dlg1 siRNA–treated cells, mean profiles were then calculated from *n* individual profiles. For both LGN and NuMA data, mean profiles were normalized through division by the mean value of the mean control profile.

To quantify the amount of LGN fusion proteins localized at the cell cortex of dividing chick neuroepithelial cells, we generated en face images of cells of interest and selected the plane of the cell largest width, corresponding to the "equator." We aimed at precisely disentangling the fluorescence signals arising from the cortex and the cytoplasm. We hypothesized that each image was a linear combination of a cortical component and a cytoplasmic component. We thus have $P = P_{cortical} + P_{cytoplasm}$, in which P is the image of the protein of interest. The cytoplasmic component was probed by the expression of an independent cytoplasmic reporter m (mRFP). Assuming that the cytoplasmic fraction of the protein of interest should adopt a similar spatial distribution as the cytoplasmic reporter, we adjusted, by a least squared optimization, the signal from the cytoplasmic reporter, measured in a small reference region (refR) of the cytoplasm distant from the cortex and the chromosomes (typically a square of 10-pixel sides), to the signal in the same region but measured for the protein of interest: $P_{refR} = \alpha \times M_{refR}$, in which M_{refR} is the image of the cytoplasmic reporter m in the reference region. The calculated proportionality coefficient α between the two signals was then used to recover the cortical component of protein p using the following operation: $P_{cortical} = P - \alpha M$, and allowing us to deduce $P_{cytoplasm}$ as well. Finally, the image $P_{cortical}$ was used to analyze 15 intensity profiles spanning the cell length, starting from the cell center and equally distributed along 360°. At this stage, most of the profiles consisted of a bell-shaped signal around the membrane location. To quantify the extent of this cortical signal, we thus fitted a Gaussian profile centered on the maximum value of the profile. The fit was performed on the four adjacent pixel values around the membrane location on each profile. The integrated intensity of the fitted Gaussian was finally calculated and interpreted as the amount of protein p cortical recruitment at the membrane location on the profile. The cytoplasmic signal on a same profile was measured on $P_{cytoplasm}$ as the integrated intensity along the same line, from the cell center to the membrane location. In the end, the ratio of cortical signal over cytoplasmic signal for each of the 15 profiles was averaged to get a final relative level of protein p recruitment at the membrane in the cell of interest.

Online supplemental material

Fig. S1 presents a characterization of chick Dlg family members' expression in the chick neural tube and the experimental validation of Dlg1

miRNA efficiency. Fig. S2 summarizes all the gain-of-function, loss-of-function, and reporter constructs used in this study. Fig. S3 shows that the direct interaction between the GUK domain of Dlg1 and the linker domain of LGN is necessary for LGN cortical localization and for planar spindle orientation in the neuroepithelium, in complement to data presented in Fig. 4. Videos show the 3D spindle movements of dividing control (Video 1) or Dlg1 knockdown (Video 2) chick neuroepithelial cells expressing H2B-GFP and PACT-mKO1 reporters of chromosomes and centrosomes. Zip file 1 contains a PDF document that explains the procedure for the successive use of two Fiji macros to perform batch measurements of mitotic spindle orientation relative to the apical surface of the tissue and the two Fiji macro files. Zip file 2 contains a PDF file describing the two MATLAB procedures and two folders containing the MATLAB code. Online supplemental material is available at http://www.jcb.org/cgi/content/full/jcb.201405060/DC1.

We thank Fumio Matsuzaki for PACT-mKO1 and the LGN antibody and Sonia Garel and Samuel Tozer for discussions and critical comments on the manuscript. We acknowledge Benjamin Mathieu and the Institut de Biologie de l'École Normale Supérieure imaging platform for excellent assistance. Imaging equipment was acquired through the generous help of the Neuropole de Recherche Francilien (NeRF).

Work in X. Morin's laboratory is supported by an Institut National de la Santé et de la Recherche Médicale Avenir grant (R08221JS), the Fondation pour la Recherche Medicale (FRM; implantation nouvelle équipe), the Fondation Association pour la Recherche contre le Cancer (ARC; ARC Livespin 2012), and the Agence Nationale pour la Recherche (ANR; ANR Blanche 2012). M. Saadaoui was the recipient of postdoctoral fellowships from the Institut National de la Santé et de la Recherche Médicale (Avenir) and NeRF. Work in A. Echard's laboratory is supported by the Institut Pasteur, the Centre National de la Recherche Scientifique, the FRM (Equipe FRM DEQ20120323707), and the Fondation ARC (to M. Machicoane). This work has received support under the program Investissements d'Avenir launched by the French government and implemented by the ANR (references: ANR-10-LABX-54 MEMO LIFE and ANR-11-IDEX-0001-02 PSL* Research University).

The authors declare no competing financial interests.

Submitted: 26 May 2014
Accepted: 7 August 2014

References

Assémat, E., E. Bazellières, E. Pallesi-Pocachard, A. Le Bivic, and D. Massey-Harroche. 2008. Polarity complex proteins. *Biochim. Biophys. Acta*. 1778:614–630. http://dx.doi.org/10.1016/j.bbamem.2007.08.029

Bellaïche, Y., A. Radovic, D.F. Woods, C.D. Hough, M.L. Parmentier, C.J. O'Kane, P.J. Bryant, and F. Schweisguth. 2001. The Partner of Inscuteable/Discs-large complex is required to establish planar polarity during asymmetric cell division in *Drosophila*. *Cell*. 106:355–366. http://dx.doi.org/10.1016/S0092-8674(01)00444-5

Bergstralh, D.T., H.E. Lovegrove, and D. St Johnston. 2013. Discs large links spindle orientation to apical-basal polarity in *Drosophila* epithelia. *Curr. Biol.* 23:1707–1712. http://dx.doi.org/10.1016/j.cub.2013.07.017

Das, R.M., N.J. Van Hateren, G.R. Howell, E.R. Farrell, F.K. Bangs, V.C. Porteous, E.M. Manning, M.J. McGrew, K. Ohyama, M.A. Sacco, et al. 2006. A robust system for RNA interference in the chicken using a modified microRNA operon. *Dev. Biol.* 294:554–563. http://dx.doi.org/10.1016/j.ydbio.2006.02.020

Elias, S., M.S. Thion, H. Yu, C.M. Sousa, C. Lasgi, X. Morin, and S. Humbert. 2014. Huntingtin regulates mammary stem cell division and differentiation. *Stem Cell Rev.* 2:491–506. http://dx.doi.org/10.1016/j.stemcr.2014.02.011

Fink, J., N. Carpi, T. Betz, A. Bétard, M. Chebah, A. Azioune, M. Bornens, C. Sykes, L. Fetler, D. Cuvelier, and M. Piel. 2011. External forces control mitotic spindle positioning. *Nat. Cell Biol.* 13:771–778.

Fleming, E.S., M. Zajac, D.M. Moschenross, D.C. Montrose, D.W. Rosenberg, A.E. Cowan, and J.S. Tirnauer. 2007. Planar spindle orientation and asymmetric cytokinesis in the mouse small intestine. *J. Histochem. Cytochem.* 55:1173–1180. http://dx.doi.org/10.1369/jhc.7A7234.2007

Guilgur, L.G., P. Prudêncio, T. Ferreira, A.R. Pimenta-Marques, and R.G. Martinho. 2012. *Drosophila* aPKC is required for mitotic spindle orientation during symmetric division of epithelial cells. *Development*. 139:503–513. http://dx.doi.org/10.1242/dev.071027

Hao, Y., Q. Du, X. Chen, Z. Zheng, J.L. Balsbaugh, S. Maitra, J. Shabanowitz, D.F. Hunt, and I.G. Macara. 2010. Par3 controls epithelial spindle orientation by aPKC-mediated phosphorylation of apical Pins. *Curr. Biol.* 20:1809–1818. http://dx.doi.org/10.1016/j.cub.2010.09.032

Iizuka-Kogo, A., T. Ishidao, T. Akiyama, and T. Senda. 2007. Abnormal development of urogenital organs in Dlgh1-deficient mice. *Development*. 134:1799–1807. http://dx.doi.org/10.1242/dev.02830

Johnston, C.A., K. Hirono, K.E. Prehoda, and C.Q. Doe. 2009. Identification of an Aurora-A/PinsLINKER/Dlg spindle orientation pathway using induced cell polarity in S2 cells. *Cell*. 138:1150–1163. http://dx.doi.org/10.1016/j.cell.2009.07.041

Johnston, C.A., D.S. Whitney, B.F. Volkman, C.Q. Doe, and K.E. Prehoda. 2011. Conversion of the enzyme guanylate kinase into a mitotic-spindle orienting protein by a single mutation that inhibits GMP-induced closing. *Proc. Natl. Acad. Sci. USA*. 108:E973–E978. http://dx.doi.org/10.1073/pnas.1104365108

Kiyomitsu, T., and I.M. Cheeseman. 2012. Chromosome- and spindle-pole-derived signals generate an intrinsic code for spindle position and orientation. *Nat. Cell Biol.* 14:311–317.

Kiyomitsu, T., and I.M. Cheeseman. 2013. Cortical dynein and asymmetric membrane elongation coordinately position the spindle in anaphase. *Cell*. 154:391–402. http://dx.doi.org/10.1016/j.cell.2013.06.010

Konno, D., G. Shioi, A. Shitamukai, A. Mori, H. Kiyonari, T. Miyata, and F. Matsuzaki. 2008. Neuroepithelial progenitors undergo LGN-dependent planar divisions to maintain self-renewability during mammalian neurogenesis. *Nat. Cell Biol.* 10:93–101.

Laprise, P., A. Viel, and N. Rivard. 2004. Human homolog of disc-large is required for adherens junction assembly and differentiation of human intestinal epithelial cells. *J. Biol. Chem.* 279:10157–10166. http://dx.doi.org/10.1074/jbc.M309843200

Lechler, T., and E. Fuchs. 2005. Asymmetric cell divisions promote stratification and differentiation of mammalian skin. *Nature*. 437:275–280. http://dx.doi.org/10.1038/nature03922

Machicoane, M., C.A. de Frutos, J. Fink, M. Rocancourt, Y. Lombardi, S. Garel, M. Piel, and A. Echard. 2014. SLK-dependent activation of ERMs controls LGN–NuMA localization and spindle orientation. *J. Cell Biol.* 205:791–799. http://dx.doi.org/10.1083/jcb.201401049

Mahoney, Z.X., B. Sammut, R.J. Xavier, J. Cunningham, G. Go, K.L. Brim, T.S. Stappenbeck, J.H. Miner, and W. Swat. 2006. Discs-large homolog 1 regulates smooth muscle orientation in the mouse ureter. *Proc. Natl. Acad. Sci. USA*. 103:19872–19877. http://dx.doi.org/10.1073/pnas.0609326103

Morin, X., and Y. Bellaïche. 2011. Mitotic spindle orientation in asymmetric and symmetric cell divisions during animal development. *Dev. Cell*. 21:102–119. http://dx.doi.org/10.1016/j.devcel.2011.06.012

Morin, X., F. Jaouen, and P. Durbec. 2007. Control of planar divisions by the G-protein regulator LGN maintains progenitors in the chick neuroepithelium. *Nat. Neurosci.* 10:1440–1448. http://dx.doi.org/10.1038/nn1984

Naim, E., A. Bernstein, J.F. Bertram, and G. Caruana. 2005. Mutagenesis of the epithelial polarity gene, discs large 1, perturbs nephrogenesis in the developing mouse kidney. *Kidney Int.* 68:955–965. http://dx.doi.org/10.1111/j.1523-1755.2005.00489.x

Nakajima, Y., E.J. Meyer, A. Kroesen, S.A. McKinney, and M.C. Gibson. 2013. Epithelial junctions maintain tissue architecture by directing planar spindle orientation. *Nature*. 500:359–362. http://dx.doi.org/10.1038/nature12335

Noatynska, A., M. Gotta, and P. Meraldi. 2012. Mitotic spindle (DIS)orientation and DISease: cause or consequence? *J. Cell Biol.* 199:1025–1035. http://dx.doi.org/10.1083/jcb.201209015

Pease, J.C., and J.S. Tirnauer. 2011. Mitotic spindle misorientation in cancer—out of alignment and into the fire. *J. Cell Sci.* 124:1007–1016. http://dx.doi.org/10.1242/jcs.081406

Peyre, E., F. Jaouen, M. Saadaoui, L. Haren, A. Merdes, P. Durbec, and X. Morin. 2011. A lateral belt of cortical LGN and NuMA guides mitotic spindle movements and planar division in neuroepithelial cells. *J. Cell Biol.* 193:141–154. http://dx.doi.org/10.1083/jcb.201101039

Postiglione, M.P., C. Jüschke, Y. Xie, G.A. Haas, C. Charalambous, and J.A. Knoblich. 2011. Mouse inscuteable induces apical-basal spindle orientation to facilitate intermediate progenitor generation in the developing neocortex. *Neuron*. 72:269–284. http://dx.doi.org/10.1016/j.neuron.2011.09.022

Quyn, A.J., P.L. Appleton, F.A. Carey, R.J. Steele, N. Barker, H. Clevers, R.A. Ridgway, O.J. Sansom, and I.S. Näthke. 2010. Spindle orientation bias in gut epithelial stem cell compartments is lost in precancerous tissue. *Cell Stem Cell*. 6:175–181. http://dx.doi.org/10.1016/j.stem.2009.12.007

Rivera, C., I.F. Yamben, S. Shatadal, M. Waldof, M.L. Robinson, and A.E. Griep. 2009. Cell-autonomous requirements for Dlg-1 for lens epithelial cell structure and fiber cell morphogenesis. *Dev. Dyn.* 238:2292–2308. http://dx.doi.org/10.1002/dvdy.22036

Sans, N., P.Y. Wang, Q. Du, R.S. Petralia, Y.X. Wang, S. Nakka, J.B. Blumer, I.G. Macara, and R.J. Wenthold. 2005. mPins modulates PSD-95 and SAP102 trafficking and influences NMDA receptor surface expression. *Nat. Cell Biol.* 7:1179–1190.

Schindelin, J., I. Arganda-Carreras, E. Frise, V. Kaynig, M. Longair, T. Pietzsch, S. Preibisch, C. Rueden, S. Saalfeld, B. Schmid, et al. 2012. Fiji: an open-source platform for biological-image analysis. *Nat. Methods*. 9:676–682. http://dx.doi.org/10.1038/nmeth.2019

Siegrist, S.E., and C.Q. Doe. 2005. Microtubule-induced Pins/Gαi cortical polarity in *Drosophila* neuroblasts. *Cell*. 123:1323–1335. http://dx.doi.org/10.1016/j.cell.2005.09.043

Théry, M., V. Racine, A. Pépin, M. Piel, Y. Chen, J.B. Sibarita, and M. Bornens. 2005. The extracellular matrix guides the orientation of the cell division axis. *Nat. Cell Biol.* 7:947–953.

Théry, M., A. Jiménez-Dalmaroni, V. Racine, M. Bornens, and F. Jülicher. 2007. Experimental and theoretical study of mitotic spindle orientation. *Nature*. 447:493–496. http://dx.doi.org/10.1038/nature05786

Willard, F.S., R.J. Kimple, and D.P. Siderovski. 2004. Return of the GDI: the GoLoco motif in cell division. *Annu. Rev. Biochem.* 73:925–951. http://dx.doi.org/10.1146/annurev.biochem.73.011303.073756

Williams, S.E., S. Beronja, H.A. Pasolli, and E. Fuchs. 2011. Asymmetric cell divisions promote Notch-dependent epidermal differentiation. *Nature*. 470:353–358. http://dx.doi.org/10.1038/nature09793

Woods, D.F., and P.J. Bryant. 1991. The discs-large tumor suppressor gene of *Drosophila* encodes a guanylate kinase homolog localized at septate junctions. *Cell*. 66:451–464. http://dx.doi.org/10.1016/0092-8674(81)90009-X

Yu, F., X. Morin, Y. Cai, X. Yang, and W. Chia. 2000. Analysis of partner of inscuteable, a novel player of *Drosophila* asymmetric divisions, reveals two distinct steps in inscuteable apical localization. *Cell*. 100:399–409. http://dx.doi.org/10.1016/S0092-8674(00)80676-5

Yu, F., X. Morin, R. Kaushik, S. Bahri, X. Yang, and W. Chia. 2003. A mouse homologue of *Drosophila* pins can asymmetrically localize and substitute for pins function in *Drosophila* neuroblasts. *J. Cell Sci.* 116:887–896. http://dx.doi.org/10.1242/jcs.00297

Zheng, Z., H. Zhu, Q. Wan, J. Liu, Z. Xiao, D.P. Siderovski, and Q. Du. 2010. LGN regulates mitotic spindle orientation during epithelial morphogenesis. *J. Cell Biol.* 189:275–288. http://dx.doi.org/10.1083/jcb.200910021

Zhu, J., Y. Shang, C. Xia, W. Wang, W. Wen, and M. Zhang. 2011. Guanylate kinase domains of the MAGUK family scaffold proteins as specific phosphoprotein-binding modules. *EMBO J.* 30:4986–4997. http://dx.doi.org/10.1038/emboj.2011.428

Žigman, M., M. Cayouette, C. Charalambous, A. Schleiffer, O. Hoeller, D. Dunican, C.R. McCudden, N. Firnberg, B.A. Barres, D.P. Siderovski, and J.A. Knoblich. 2005. Mammalian inscuteable regulates spindle orientation and cell fate in the developing retina. *Neuron*. 48:539–545. http://dx.doi.org/10.1016/j.neuron.2005.09.030